RSC Advances

RSC Publishing

PAPER

View Article Online
View Journal | View Issue

A microporous titanosilicate for selective killing of HeLa cancer cells†

Cite this: *RSC Advances*, 2013, **3**, 8843

Received 18th December 2012,
Accepted 28th March 2013

DOI: 10.1039/c3ra23381b

www.rsc.org/advances

Stanislav Ferdov,*[a] Evelina Shikova,[bc] Zina Ivanova,[b] Louiza T. Dimowa,[d] Rositsa P. Nikolova,[d] Zhi Lin[e] and Boris L. Shivachev[d]

Structural distribution of zinc(II) ions in the pore system of three silicate molecular sieves has revealed an unprecedented application of the microporous titanosilicate Zn ETS 4 as a non toxic, highly efficient and selective inhibitor of HeLa cancer cells.

1 Introduction

On an industrial scale, zeolites and related porous materials have been extensively used as catalysts, ion exchangers, adsorbents and detergent builders. Due to their ability for reversible binding of small molecules such as oxygen and nitric oxide alternative applications in medicine and pharmacy have been also revealed.[1–3] The size and shape selectivity of the variety of microporous frameworks offer possibilities of metalloenzyme mimicry, immunomodulatory activity,[4] as well as antibacterial and antiviral applications.[5–9] Metal-exchanged (Zn^{2+}, Ag^{+}, Cu^{2+}) forms of microporous solids have been also explored for active carriers of antibiotics and antimicrobial applications.[10–13] Medical investigations of zeolites as anti-tumor agents are only known for mechanically treated natural zeolite clinoptilolite that has been applied to several cancer models.[3] However, the strongest inhibition is achieved for mouse fibrosarcoma cells, and for HeLa (human cervical carcinoma cell line) cancer cells the reported value is less than 50%. In medicine, the antitumor effect of the Zn^{2+} ion is well known,[14–17] however the problem with the discrimination between the cancer and the healthy cells remains one of the most important challenges.[18,19] Here, we show that Zn^{2+} ions included in the pore system of the microporous titanosilicate ETS-4 (Engelheart titanium silicate-4),[20] transform the material to a highly efficient and selective inhibitor of HeLa cancer cells. The obtained solid (Zn–ETS-4), without affecting the healthy cells, can reduce the tumor cells down to 5%. These results are compared to another Zn-exchanged microporous titanosilicate (STS-Sofia titanium silicate, also known as AM-2-Aveiro-Manchester or synthetic umbite)[21,22] and natural clinoptilolite (CPT), which demonstrated that the specific host of incorporation of Zn^{2+} is important for the efficiency and selectivity of the antitumor effect. All these materials have also been tested against HepG2 (human hepatocellular carcinoma cell line) cancer cells, indicating a lower efficiency but still superior cytotoxicity of Zn–ETS-4. Our findings discover new options for application of the metal exchanged zeolites and mixed tetrahedral–octahedral molecular sieves.

2 Experimental section

2.1 Synthesis and ion exchange

ETS-4 and STS were synthesized according to a previously reported procedure.[23] For structural determination and elucidation of the positions of the Zn^{2+} ions, single crystals of ETS-4 have been prepared.[24] The source of natural clinoptilolite (CPT) was the deposit of Beli plast, Kardzhali, Bulgaria. The ion exchange was performed by immersing the as-synthesized ETS-4, STS and CPT in 1 M solutions of $ZnCl_2$ (Aldrich) for 3 days at 90 °C (30 days at 100 °C for CPT). Finally, the samples were washed several times (5–7) by distilled water (around 300 ml H_2O per 0.5 g of solid product) and dried at room temperature.

2.2 Characterization

The chemical composition was ascertained by energy-dispersive X-ray spectroscopy (EDAX-Pegasus X4M (EDS/EBSD) and Zeiss LS 25) and inductively coupled plasma (ICP-Varian Vista MPX CCD). The images were taken by NanoSEM-FEI Nova 200

[a]*Department of Physics, University of Minho, 4800 058 Guimaraes, Portugal. E mail: sferdov@fisica.uminho.pt; Fax: +351 253 510 461; Tel: +351 253 510 468*
[b]*Institute of Experimental Morphology, Pathology and Anthropology with Museum, Bulgarian Academy of Sciences, Sofia, 1113, Bulgaria*
[c]*National Center of Infectious and Parasitic Diseases, General Stoletov Str. 44A, 1233 Sofia, Bulgaria*
[d]*Institute of Mineralogy and Crystallography, Bulgarian Academy of Sciences, Sofia, 1113, Bulgaria*
[e]*CICECO, University of Aveiro, 3810 193 Aveiro, Portugal*

† Electronic supplementary information (ESI) available: Details on the crystal structure analyses may be obtained from the Fachinformationszentrum Karlsruhe, 76344 Eggenstein Leopoldshafen, Germany (fax: (+49) 7247 808 666; e mail: crysdata@fiz karlsruhe.de), on quoting the depository numbers ICSD: 425338 (Zn STS), ICSD: 425339 (Zn CPT), and ICSD: 425400 (Zn ETS 4). The cif files and the parameters of the refined structures are also available in the supporting information. SEM images, chemical and TGA analyses are also included. See DOI: 10.1039/c2ra23381b

(FEG/SEM). The amount of hydroxyl species was determined by thermogravimetry analyses (TGA) using Shimadzu TG-50 (in air at the rate of 5 °C min $^{-1}$) and Stanton Redcroft (in argon at the rate of 5 °C min $^{-1}$, 30–700 °C) analyzers. The powder XRD analyses were collected on Bruker D8 Discover and Bruker D8 Advance diffractometers (Cu-Kα radiation, λ = 1.5406 Å). The single crystal data were collected on an Agilent Diffraction SuperNovaDual four-circle diffractometer equipped with an Atlas CCD detector using mirror-monochromatized Mo-Kα radiation from a micro-focus source (λ = 0.7107 Å).

2.2.1 Crystal data for $K_{1.16}Zn_{0.42}TiSi_3O_9 \cdot 2H_2O$ (Zn–STS). M = 1469.96 g mol $^{-1}$, monoclinic space group: $P2_1/c$ (14), a = 7.205(9), b = 10.034(2), c = 12.89(4) Å, β = 91.5(1)°, V = 931.9(9) Å^3, ρ_c = 2.6189(1) g cm $^{-3}$, R_p = 8.25, R_{wp} = 11.08, R_{exp} = 4.44, χ^2 = 2.49, R_B = 4.31.

2.2.2 Crystal data for $(Na_{0.2}Ca_{0.4}K_{0.4}Mg_{0.2})Zn_{2.2}Al_6Si_{30}O_{72} \cdot 19H_2O$ (Zn–CPT). M = 2646.68 g mol $^{-1}$, monoclinic space group: $C2/m$ (12), a = 17.648(9), b = 17.963(1), c = 7.405(7) Å, β = 116.2(4)°, V = 2105.8(5) Å^3, ρ_c = 2.0868(8) g cm $^{-3}$, R_p = 4.17, R_{wp} = 5.39, R_{exp} = 2.92, χ^2 = 1.83, R_B = 1.53.

2.2.3 Crystal data for $Zn_{3.15}H_{4.76}Si_{12}Ti_5O_{39} \cdot 6.6H_2O$ (Zn–ETS-4). M = 1510.1(1) g mol $^{-1}$, orthorhombic space group: $Cmmm$ (65), a = 22.879(6), b = 7.2161(15), c = 6.765(2) Å, V = 1116.8(5) Å^3, ρ_c = 2.2450(4) g cm $^{-3}$, μ(Mo-Kα) = 2.913 mm $^{-1}$, R_1 = 0.127, wR_2 = 0.292 (all data).

2.2.4 Cell cultures. The cell lines from hepatocellular carcinoma (HepG2), cervical carcinoma (HeLa) and the non-tumor cell line of murine fibroblasts (3T3) were used in this study. The cells were grown in Dulbecco's Modified Eagle's Medium (DMEM, Gibco-Invitrogen, UK) supplemented with 10% fetal calf serum (Gibco-Invitrogen, UK), 100 U ml $^{-1}$ penicillin and 100 μg ml $^{-1}$ streptomycin. All cell lines were maintained at 37 °C in a 5% CO_2 incubator. Cells were subcultured regularly using trypsin–EDTA. All of the experiments were carried out in the exponential phase of cell growth.

2.2.5 Cytotoxicity assay. A neutral red (NR) cytotoxicity assay based on the protocol described by Borenfreund and Puerner[25] was carried out. Briefly, cells were seeded in 96-well microtiter plates (Scientific Orange) at 10^5 cells/well and allowed to attach overnight. The cells were then treated for 24 h with different concentrations of each zeolite: 0.667 mg ml $^{-1}$, 0.445 mg ml $^{-1}$, 0.296 mg ml $^{-1}$, 0.198 mg ml $^{-1}$, 0.132 mg ml $^{-1}$, 0.088 mg ml $^{-1}$, 0.058 mg ml $^{-1}$ and 0.039 mg ml $^{-1}$. For the cytotoxicity assay, 100 μl of NR solution (50 μg ml $^{-1}$) was added to each well. After 3 h incubation at 37 °C and 5% CO_2, cells were destained with 100 μl of acetic acid (1%)–ethanol (50%) (v/v). Untreated cells were used as controls, and wells with a culture medium without cells were used as blank controls. The optical density was measured at 570 nm with a microplate reader (TECAN, SunriseTM, Austria). The viability was represented as the percentage of viable cells after preincubation with zeolites, as compared to the untreated control group and was calculated for each concentration. The percentage of inhibition of the cells was estimated as follows: Cell viability (%) = OD570 (experimental)/OD570(control) × 100. All experiments were performed in triplicate.

2.2.6 Statistical analysis. The results from treated and control cells were compared using one-way analysis of variance (ANOVA) followed by a Dunnett test. A P-value < 0.05 was considered statistically significant. The concentration of each zeolite which showed 50% cytotoxicity (IC50) was calculated. The data were analyzed using GraphPad Prizm, GraphPad Software Inc., USA, 2000. To identify statistically significant differences, results were analyzed by the analysis of variance using Dunnet's Multiple Comparison Test. Probability values of $*p < 0.05$, $**p < 0.01$, and $***p < 0.001$ were considered significant.

3 Results and discussion

3.1 Cytotoxic activity

In vitro cytotoxic activities of Zn–ETS-4, Zn–STS, Zn–CPT and CPT have been tested by NR (neutral red) assay using HeLa and HepG2 tumor cell lines and non-tumor cell line 3T3. NR is a weak cationic dye that incorporates into the lysosomes of living cells but not of damaged cells. Therefore the NR assay provides a quantitative estimation of the number of viable cells. Zn–CPT and Zn–ETS-4 showed significant cytotoxicity (Fig. 1) to HeLa cells, when compared to the controls ($P < 0.05$ for each, one-way ANOVA). The IC50 values of Zn–CPT and Zn–ETS-4 were 0.405 mg ml $^{-1}$ and 0.543 mg ml $^{-1}$, respectively. Zn–CPT and Zn–ETS-4 exhibited high cytotoxic activity in a very narrow concentration range—there was no reduction in cell viability at lower concentrations but significant reduction was induced at concentrations above 0.445 mg ml $^{-1}$. At the highest concentration (0.667 mg ml $^{-1}$), about 95% loss of cell viability was registered, however, cells remained more than 85% and 33.6% viable relative to the controls at concentration 0.445 mg ml $^{-1}$ of Zn–ETS-4 and Zn–CPT, respectively. The same materials applied to the HepG2 tumor cell line showed lower cytotoxic activity. The viability of HepG2 cells treated with Zn–ETS-4 was only slightly decreased—cells remained more than 72% viable relative to controls, suggesting that Zn–ETS-4 had low cytotoxicity to HepG2 cells, even at the highest concentration of 0.667 mg ml $^{-1}$. Zn–CPT did not affect the HepG2 cell viability, indicating no cytotoxicity to this cancer cell line. For comparison, we also determined the cytotoxicity of each solid against non-tumor mammalian cells (3T3 cell line). Zn–CPT induced 28% loss of 3T3 cell viability. No cytotoxicity of Zn–ETS-4 was observed to non-tumor 3T3 cells up to the highest concentration of 0.667 mg ml $^{-1}$, demonstrating high selectivity towards the tumor cells.

The natural non-modified CPT and the Zn-exchanged STS did not affect the cell viability at all concentrations in all cell lines used in the study, showing that they have no cytotoxic activity (Fig. 1).

The obtained results clearly indicate that Zn–CPT can be applied for selective inhibition of HeLa cancer cells while sparing the HepG2 cells (Fig. 1). However, nowadays one of the most important challenges is the development of anticancer agents that can target cancer cells without affecting the healthy tissue. In this aspect, Zn–ETS-4 shows more promising behavior as it can suppress at the same time both cancer cell lines (HeLa and HepG2), and in certain concentrations it reduces the HeLa cancer cells down to 5% without any cytotoxicity to the non-tumor cells of the 3T3 cell line.

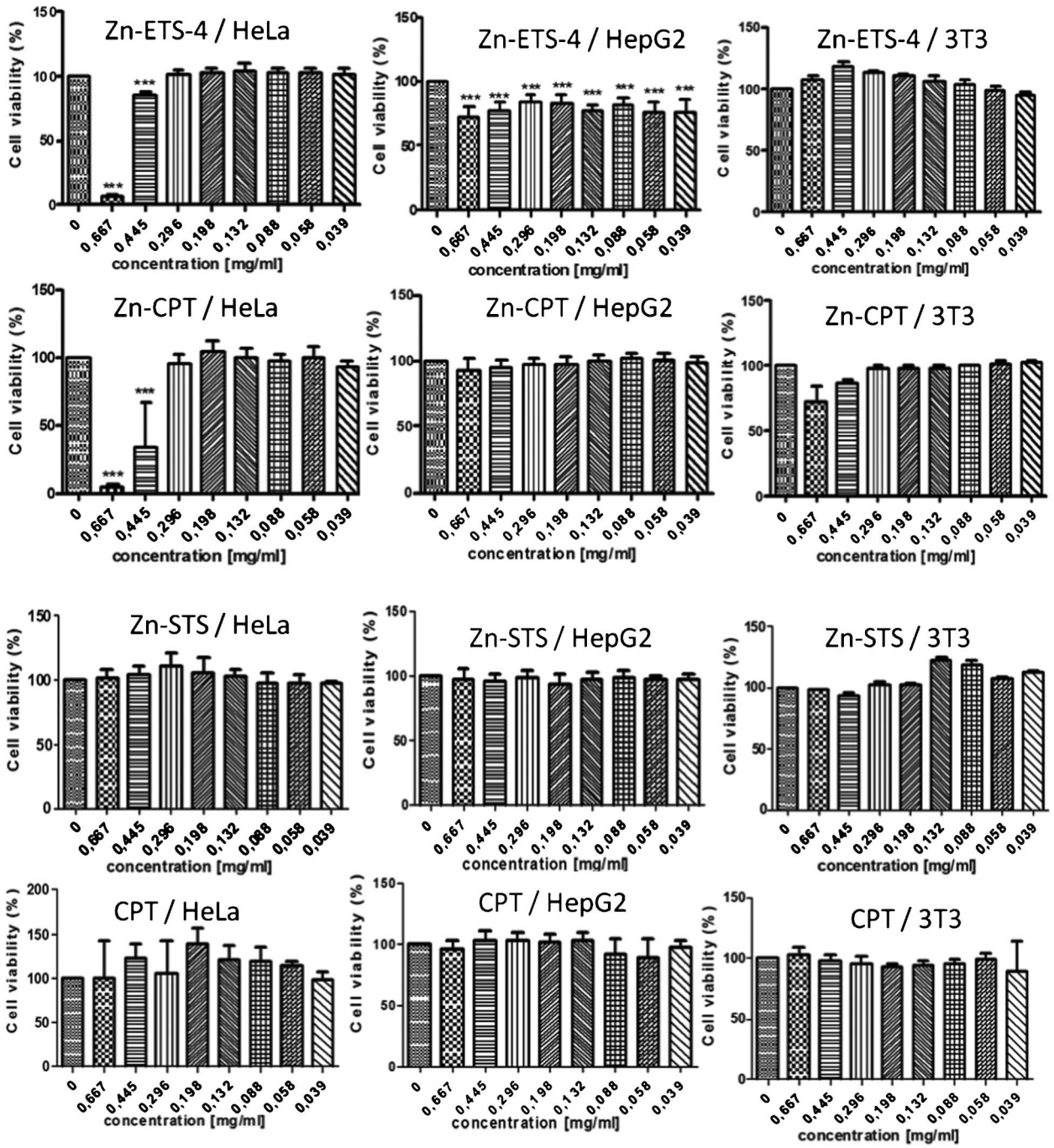

Fig. 1 Cell viability of HeLa, HepG2 and 3T3 cell lines assessed by the neutral red (NR) incorporation method. The molecular sieves Zn ETS 4, Zn CPT, Zn STS and CPT were added at concentrations shown in the graphics (0.667 to 0.039 mg ml^{-1}) for 24 h. The NR assay was then performed. The relation between sample absorbance and control absorbance calculated the relative absorbance.

3.2 Crystal structure and zinc ion distribution of Zn–STS

A key to understanding antitumor properties is the interaction of the Zn^{2+} ion with the microporous host. X-ray diffraction is sensitive to local compositional and structural changes and therefore provides insight into the possible reasons for the different antitumor behaviour. Thus, upon ion exchange with Zn^{2+}, the crystal symmetry of STS changes from orthorhombic ($P2_12_12_1$) to monoclinic ($P2_1/c$). This type of conversion has been previously described for other ion exchanged forms of metal silicates with an umbite-like structure.[26–28] The inclusion of Zn^{2+} does not change the framework topology and it remains a three-dimensional mixed framework with six- and eight- ring channels. The primary building units are three independent silicon atoms forming a trisilicate group Si_3O_9, interconnected by one six coordinated (TiO_6) titanium atom.

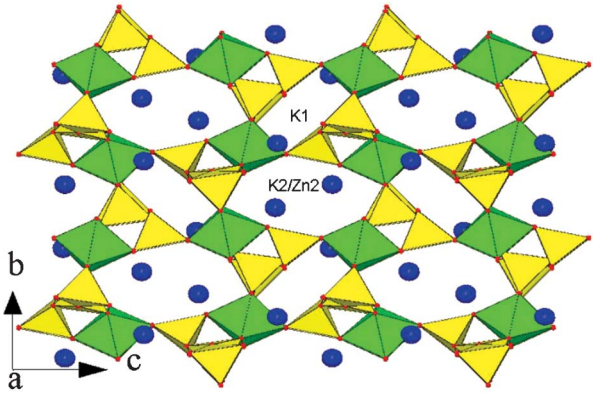

Fig. 2 Crystal structure of Zn STS. SiO_4 tetrahedra are bright (yellow) colored, Ti octahedra are light (green) colored. For clarity the water molecules are omitted.

The ion exchange with Zn^{2+} altered the content and atomic distribution in the voids. The electronic density over the 6-ring channels showed one fully occupied K^+ ion suggesting a lower susceptibility for replacement. Analysis of site occupancy and bond distances indicated that Zn^{2+} has an affinity to locate in the bigger 8-ring channels where it partly substitutes K^+ with a composition of 0.42 Zn and 0.16 K (Fig. 2). In the same channel the water molecules are found unevenly distributed over the cation site and the two water positions. The high isotropic parameters and some short Zn–Ow1 (1.711(4) Å) and Ow1–Ow2 (water molecules) bond distances (1.781(1) Å) suggest highly disordered Zn/H_2O distribution. Considering the presence of surface water, the detected 10.5% weight loss is not far from the expected 2 water molecules per formula unit (calculated 9.3%).

3.3 Crystal structure and zinc ion distribution of Zn–CPT

The natural CPT from Beli plast (Bulgaria) is well studied and a comparison with previously published data[29] indicated that the ion exchange with Zn^{2+} did not change the framework characteristics. Two Zn^{2+} sites (Zn1 and Zn3) in the 10-ring channels and one (Zn2) in the 8-ring channels (Fig. 3) have been found.[30] Six independent sites corresponding to water molecules have been also located. Two of them are situated in the 8-ring and the other four are in the bigger 10-ring channels.[27] The refinement of the structure allowed the detection of 18.98 water molecules per formula unit, however the total weight loss of 14.44% pointed to more hydroxyl species whose structural assignment was not possible.

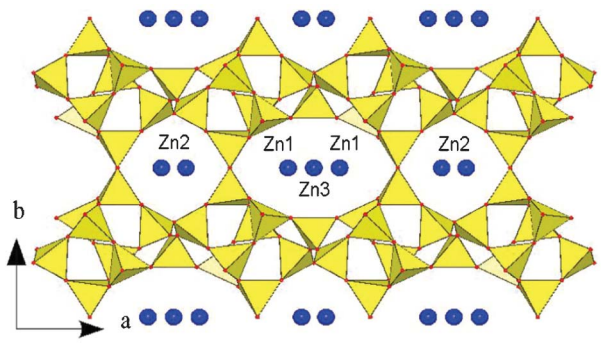

Fig. 3 Crystal structure of Zn CPT. Si/Al tetrahedra are bright (yellow) colored. For clarity the water molecules are omitted.

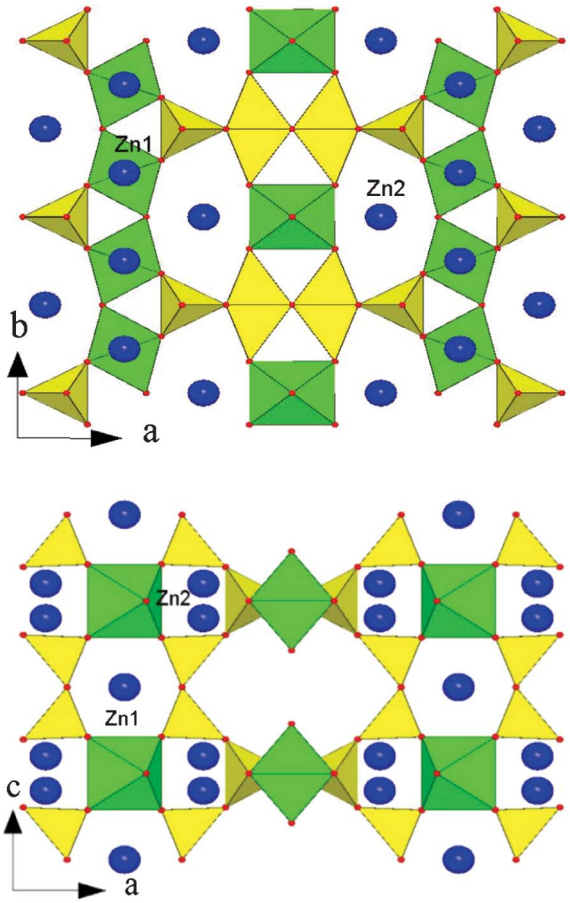

Fig. 4 Crystal structure of Zn ETS 4 projected along *c* (up) and *b* (down) axes. SiO_4 tetrahedra are bright (yellow) colored, Ti octahedra are light (green) colored. For clarity the water molecules are omitted.

3.4 Crystal structure and zinc ion distribution of Zn–ETS-4

The framework of ETS-4 is composed of chains of corner sharing TiO_6 octahedra running along the *b*-axis. These chains are connected by SiO_4 tetrahedra (along the *c*-direction) and titanosilicate bridging units (along the *a*-axis) (Fig. 4). The units are statistically distributed and determine the random intergrowth of the four polymorphs that compose the framework of ETS-4.[31] The bridging units contain isolated titanium atoms whose coordination environment has attracted various studies. Originally, the single crystal X-ray diffraction study from the natural analogue of ETS-4 indicated that mineral zorite[32] has a bridging unit composed of titanium semi-octahedra where the Ti–O distance varies between 2.02 Å for the basal and 1.67 Å for the apical oxygens. A later single crystal investigation of Na–ETS-4[33] confirmed the five coordinated titanium where the Ti–O distance varies between 1.96 Å and 1.70 Å, respectively. The powder X-ray diffraction

investigation of Na–ETS-4[34] and Sr–ETS-4[31] gave controversial conclusions about the six-coordination of the titanium in the bridging unit. While the Na–ETS-4 was claimed to have six-coordinated titanium, in Sr–ETS-4 it was confirmed to have five-coordinated titanium from the single crystal data. A recent single crystal study of Ba-exchanged ETS-4 again suggested the possibility of six-coordinated titanium in the bridging unit.[24] Our results showed that Zn-exchanged crystals of ETS-4 possess titanosilicate bridging units where the titanium (Ti2) is situated in the mirror plane (0, 0, ½) and it has 50% occupancy. It is coordinated by O5 (x, y, ½) and O7 (0, 0, z). The occupancy of O5 is ½ as is the bridging Si2, while the apical O7 occupies ¼ of the position. Thus, Ti2 can be considered as five-coordinated. In the porous system of ETS-4 there are two independent cation positions.[28–32] The first one (Zn1) is situated in the 6-ring opening formed between two TiO_6 chains, and the second one (Zn2) is in the 7-ring channel formed between the titanosilicate bridging units and TiO_6 chains (Fig. 4). No Zn atoms are positioned in the 8-ring channels propagating along the *b*-axis. Zn1 has an occupancy of 0.85 and Zn2 of about 0.18. This means that around the bridging units there are highly charged unsaturated zones and charge-balancing protons are required. Similarly to Na1 in Na–ETS-4,[33,34] Zn1 is eight-coordinated by two water molecules and six oxygens. However, Zn2 shows coordination of five oxygens which differ from the seventh coordination observed for this position in the Sr– and Na–ETS-4.[31,34] The water molecules in Zn–ETS-4 occupy three sites that are disordered over the 6-ring openings (O21) and the 8-ring channels (O22 and O23), corresponding to 6.62 water molecules per formula unit (8%). This amount is less than the estimated 12.6% weight loss which supports the presence of a number of hydrogen connected oxygens.

The obtained results clearly indicate that the complete ion exchange without a full population of Zn^{2+} ions can introduce charge unsaturated zones within the structure of ETS-4. This can bring a partial collapse of the defected framework units (titanosilicate bridging units) and as a result polymorph enriched zones are formed. This suggestion is supported by the powder XRD pattern of Zn–ETS-4 (Fig. S5, ESI†) whose extra reflections can be assigned to the previously reported orthorhombic polymorph of the phase.[31]

The structural elucidation showed that the increased amount of incorporated Zn^{2+} ions per formula unit (ETS-4 (13.4 wt.%) > STS (7.13 wt.%) > CPT (5.63 wt.%)) is not proportional to the efficiency and selectivity of the anticancer process. The material with the intermediate amount of Zn^{2+} showed no effect on the cancer cells used and the solids with the lowest and highest quantity of Zn^{2+} demonstrated a similar efficiency but different selectivities against HeLa cells. While Zn–CPT is the most efficient, Zn–ETS-4 is the most selective inhibitor of HeLa cancer cells. These findings indicate the major role of specific host accommodation of Zn^{2+} for the efficiency and selectivity of the antitumor process. In the literature the antitumor effect of the Zn^{2+} ion is well known, however the exact mechanism of action is not completely understood. There are reports suggesting that zinc may protect normal cells against DNA-damaging action and increase this action in cancer cells, which indicates the dual action of this element in the dependency on target cells.[35] From our results it is clear that the specific host accommodation of Zn^{2+} ions can provide selective cytotoxicity towards certain cancer cell lines. The zinc ion in ETS-4 occupies two positions and resides in relatively narrow channels when compared to STS and CPT. This can be a clue as to where to further search for proper carriers of metal ions.

To date, the zeolite based treatment of cancer cells is limited to natural micronized clinoptilolite, showing influence on the proliferation and survival of cancer cell lines of human origin.[3] It is suggested that clinoptilolite inhibited cell proliferation due in part to the induction of inhibitors of cyclin-dependent kinases, inhibition of B/Akt expression, induced expression of p21WAF1/CIP1 and p27KIP1 tumor suppressor proteins, and subsequent programmed cell death.[3,36] However, in our work the non-modified natural clinoptilolite did not show any cytotoxic activity (Fig. 1) which can originate from differing particle size or chemical composition. The natural origin of the CPT presumes a chemical composition determined by the specific conditions of the deposit and for better understanding of the observed effect further cytotoxic studies should be performed on synthetic molecular sieves.

4 Conclusions

In this study we extend the known applications of the metal exchanged molecular sieves by introducing the selective anticancer effect of a Zn^{2+} loaded microporous host. A crystal structure study and *in vitro* tests on cancer (HeLa, HepG2 cell lines) and non-cancer (3T3 cell line) cells reveal that the specific microporous system tends to control the selectivity and efficiency of the anticancer properties of the zinc ion. Thus, Zn^{2+} incorporated in the six- and seven-ring channels of ETS-4 transform the solid into a highly selective and efficient inhibitor of HeLa and HepG2 cancer cells, while sparing the healthy ones. On the contrary, the zinc ions in the eight- and ten-ring channels of the clinoptiolite convert the solid to an efficient but not selective inhibitor of HeLa cancer cells. Zinc exchanged eight-ring channels of STS and non exchanged clinoptiolite show no influence on the studied cancer cell lines. We anticipate that the presented results will instigate studies on other cancer genotypes targeted by various metal exchanged molecular sieves.

Acknowledgements

This work was supported by FCT, project PTDC/CTM/108953/2008.

Notes and references

1 M. Garces, *Observation of zeolite applications*, ed. M. J. Treacy, B. K. Marcus, M. E. Misher and J. B. Higgins, Proc. of the 12th Int. Conf. on Zeolites., Mater. Res. Soc., Warrendale, Penn., USA, 1999, pp. 551–566.

2 C. Colella, *Stud. Surf. Sci. Catal.*, 1999, **125**, 641.
3 M. L. Pinto, J. Rocha, J. R. B. Gomes and J. Pires, *J. Am. Chem. Soc.*, 2011, **133**, 6396.
4 K. Pavelić, M. Hadzija, L. Bedrica, J. Pavelić, I. Dikić, M. Katić, M. Kralj, M. H. Bosnar, S. Kapitanović, M. Poljak-Blazi, S. Krizanac, R. Stojković, M. Jurin, B. Subotić and M. Colić, *J. Mol. Med.*, 2001, **78**, 708.
5 G. N. Kirov and G. Terziyski, *Comparative study of clinoptilolite and zeolite A as antimicrobial agents*, ed. G. Kirov, L. Filizova and O. Petrov, Natural Zeolites, Sofia'95, Pensoft, Sofia, Bulgaria, 1995, pp. 133–141.
6 T. Yamamoto, M. Uchida and Y. Kurihara, *Zeolites*, 1997, **18**, 235.
7 A. Leophairatana and K. Yamada, *Corporate Environmental Report (FinalReport)*, ESM 210, Shiseido, LTD, 2002, May 30.
8 M. Grce and K. Pavelic, *Microporous Mesoporous Mater.*, 2005, **79**, 165.
9 T. Maeda and Y. Nose, *Artif. Organs*, 1999, **23**, 129.
10 G. Cerria, M. de Gennaro, M. C. Bonferonic and C. Caramella, *Appl. Clay Sci.*, 2004, **27**, 141.
11 P. Kaali, M. M. Pérez-Madrigal, E. Strömberg, R. E. Aune, Gy. Czél and S. Karlsson, *eXPRESS Polym. Lett.*, 2011, **5**, 1028.
12 N. J. Coleman, S. P. Lewis, A. P. Mendham and V. Trivedi, *J. Porous Mater.*, 2010, **17**, 747.
13 J. Pérez-Carvajal, P. Lalueza, C. Casado, C. Téllez and J. Coronas, *Appl. Clay Sci.*, 2012, **56**, 30.
14 Z. Ma, Y. Cao, Q. Li, M. F. C. Guedes da Silva, J. J. R. Frausto da Silva and A. J. L. Pombeiro, *J. Inorg. Biochem.*, 2010, **104**, 704.
15 D. Magda, Ph. Lecane, Z. Wang, W. Hu, P. Thiemann, X. Ma, P. K. Dranchak, X. Wang, V. Lynch, W. Wei, V. Csokai, J. G. Hacia and J. L. Sessler, *Cancer Res.*, 2008, **68**, 5318.
16 P. Feng, T. L. Li, Z. X. Guan, R. B. Franklin and L. C. Costello, *Ann. N. Y. Acad. Sci.*, 2003, **1010**, 316.
17 P. F. Liguori, A. Valentini, M. Palma, A. Bellusci, S. Bernardini, M. Ghedini, M. L. Panno, C. Pettinari, F. Marchetti, A. Crispini and D. Pucci, *Dalton Trans.*, 2010, **39**, 4205.
18 J. W. Rasmussen, E. Martinez, P. Louka and D. G. Wingett, *Expert Opin. Drug Delivery*, 2010, **7**, 1063.
19 A. B. Pardee and L. J. James, *Proc. Natl. Acad. Sci. U. S. A.*, 1975, **72**, 4994.
20 S. M. Kuznicki, *U.S. Pat.*, 4938939, 1990.
21 S. Mintova and V. Valtchev, *Bulg. Pat. Appl.*, 1996, March 29, **100**, 465.
22 Z. Lin, J. Rocha, P. Brandao, A. Ferreira, A. P. Esculcas and J. D. Pedrosa de Jesus, *J. Phys. Chem. B*, 1997, **101**, 7114.
23 V. Kostov-Kytin, S. Ferdov, Yu. Kalvachev, B. Mihailova and O. Petrov, *Microporous Mesoporous Mater.*, 2007, **105**, 232.
24 R. P. Nikolova, B. L. Shivachev and S. Ferdov, *Microporous Mesoporous Mater.*, 2013, **165**, 121.
25 E. Borenfreund and J. A. Puerner, *J. Tissue Cult. Methods*, 1984, **9**, 7.
26 A. I. Bortun, L. N. Bortun, D. M. Poojary, O. Xiang and A. Clearfield, *Chem. Mater.*, 2000, **12**, 294.
27 S. Fewox and A. Clearfield, *J. Phys. Chem. A*, 2008, **112**, 2589.
28 N. Doeblin and T. Armbruster, *Microporous Mesoporous Mater.*, 2007, **99**, 279.
29 L. Dimova, B. L. Shivachev and R. P. Nikolova, *Bulg. Chem. Commun.*, 2011, **43**, 217–224.
30 L. Dimova, *Powder X-Ray diffraction study of clinoptilolite modified by ion-exchange and occlusion*, Ph.D. Dissertation, Bulgarian Academy of Sciences, IMC-BAS, 2011.
31 C. M. Braunbarth, H. W. Hillhouse, S. Nair and M. Tsapatsis, *Chem. Mater.*, 2000, **12**, 1857.
32 P. A. Sandomirskii and N. V. Belov, *Sov. Phys. Crystallogr.*, 1979, **24**, 686.
33 S. Nair, H.-K. Jeong, A. Chandrasekaran, C. M. Braunbarth, M. Tsapatsis and S. M. Kuznicki, *Chem. Mater.*, 2001, **13**, 4247.
34 G. Cruciani, P. D. Luca, A. Nastro and P. Pattison, *Microporous Mesoporous Mater.*, 1998, **21**, 143.
35 T. Sliwinski, A. Czechowska, M. Kolodziejczak, J. Jajte, M. Wisniewska-Jarosinska and J. Blasiak, *Cell Biol. Int.*, 2009, **33**, 542.
36 N. Zarkovic, K. Zarkovic, M. Kralj, S. Borovic, S. Sabolovic, M. P. Blazi, A. Cipak and K. Pavelic, *Anticancer Res.*, 2003, **23**, 1589.